Sensoring hydrogen gas concentration using electrolyte made of proton conductive manganese dioxide

Yoshikatsu Ueda[1], Alexander I. Kolesnikov[2] and Hideki Koyanaka[3*]

[1]*Research Institute for Sustainable Humanosphere, Kyoto University, Kyoto, 611-0011, Japan*

[2]*Neutron Scattering Sciences Division, Oak Ridge National Laboratory, Oak Ridge, TN 37831-6473, USA*

[3]*Institute for Integrated Cell-Material Sciences, Kyoto University, Kyoto, 606-8501, Japan*

Email Address: yueda@rish.kyoto-u.ac.jp (Y. Ueda)

kolesnikovai@ornl.gov (A. I. Kolesnikov)

koyanaka@icems.kyoto-u.ac.jp (H. Koyanaka)

[*]Corresponding author: H. Koyanaka

ABSTRACT

Hydrogen gas promises to be a major clean fuel in the near future. Thus, sensors that can measure the concentrations of hydrogen gas over a wide dynamic range (*e.g.*, 1-99.9%) are in demand for the production, storage, and utilisation of hydrogen gas. However, it is difficult to directly measure hydrogen gas concentrations greater than 10% using conventional sensor [1-11]. We report a simple sensor using an electrolyte made of proton conductive manganese dioxide that enables in-situ measurements of hydrogen gas concentration over a wide range of 0.1-99.9% at room temperature.

1. Introduction

Manganese dioxide (MnO_2) crystallizes into various phases, including R-type ramsdellite, α-type hollandite, β-type pyrolusite, λ-type spinel, ε-type hexagonal, and γ-type nsutite, *etc*. This variation in crystal structure gives rise to a variety of very intriguing physical and chemical functions. Such functions have been using for industrial fields widely in applications of battery, adsorbent, ion-exchanger, and oxidizer, etc. In this study, a high-purity, ramsdellite-crystal type MnO_2 (RMO) [12,13] was used for an electrolyte in a hydrogen gas (H_2) sensor. The sensor system consists of the electrolyte and platinum mesh electrodes attached to the electrolyte surface, which also functioned as catalysts as in typical solid oxide fuel cell (SOFC) systems. The sensoring capability was examined for in-situ measurements of H_2 concentration over a wide range of 0.1-99.9% at room temperature.

2. Experimental

The RMO was prepared according to a previously reported method [12]. Transmission electron microscopy (TEM), X-ray diffraction (XRD) and a nitrogen gas (N_2 99.9%) adsorption method were used for sample characterisations. The RMO powder (0.6 g) was processed into a pellet (diameter: 2 cm, thickness: 0.6 mm) to act as the electrolyte in the sensor for the measurement of H_2 concentrations. And

distilled water (0.4 mL) was added onto the surface of the RMO pellet before supplying H_2. For comparison of the properties using electrolytes made of different MnO_2 crystal types, chemicals of Soekawa 02320B and Wako 134-12301 were used as the γ-MnO_2 and the commercial MnO_2, respectively. The λ-MnO_2 and the β-MnO_2 were prepared according to methods [14,15]. In addition, a titanium oxide TiO_2 (Wako 325-38392) and an activated aluminum oxide Al_2O_3 (Wako 010-01525) were tested as electrolyte pellets for comparison with MnO_2 pellets.

Fig. 1a shows a schematic of the sensor, where the platinum (Pt) meshwork pieces attached to each side of the wide pellet served as the electrodes and also as catalysts for the $H_2 \rightarrow 2H^+ + 2e^-$ dissociation. This sensor system is conceptually similar to that of a typical SOFC system. We determined voltages generated between the Pt electrodes as a function of the H_2 concentration. **Fig. 1b** shows a TEM image of aggregated nano-particles of the RMO growing along a specific crystal axis. The meso-space between the aggregated nano-particles was estimated to be about 20 nm, which is large enough for the infiltration of air and water molecules. The surface area was found to be 71.2 m^2/g. The proton conductivity of the RMO was examined by using alternative current (AC) impedance method.

3. Results and discussion

Fig. 2a shows the output voltages between the Pt electrodes with the sequential supply of H_2 and N_2 to the cathode surface of the electrolyte pellet (N_2 was used to purge H_2 from the cathode). Exposing the electrolyte to 0.1% and 50% of H_2 clearly produced quick responses, within 0.5 sec, in the output voltage, corresponding to the supply and purge of H_2.

Fig. 2b shows the dependence of the output voltage on the H_2 concentration and the response (*i.e.*, dV/dt) on the left and the right sides of the vertical axis, respectively. A saturation of output voltages was observed for H_2 concentrations greater than 10%. However, the response showed linearity from 0.1% to 99.9% H_2 with a correlation coefficient of 0.99 for the best-fit line. Thus, the best-fit line of dV/dt can be used as the standard curve to calculate unknown concentrations of H_2 in a sample gas. The

sensor showed a stable performance in the current experiment which lasts over 2 years period; however the wetness of the electrolyte should be maintained at least 0.3 g water / 1 g RMO. Thus, the wetness control of the electrolyte will be required to this sensoring system for the industrial utilization.

Moreover, we determined the sensor properties using electrolytes made of different MnO_2 crystal types (XRD patterns of tested MnO_2 are shown in see Supplementary data S1.), and the results are compared in **Table 1**. The RMO (Sample no. 1; R-type, orthorhombic structure [16]) showed the highest response and lowest residual voltage (*i.e.*, the voltage that remained after purging H_2 from the cathode surface with N_2). The different results between the RMO and the γ-type MnO_2 (Sample no. 2; R-type containing β-type rutile structure [17] and ε-type hexagonal structure [18] as the inter growths in the orthorhombic structure [19]) indicate that the purity of R-type crystal is an important factor to obtain the low residual voltage in the sensor for the measurement of H_2 concentrations. Thus, the commercial MnO_2 (Sample no. 3) which contains other different crystals in the structure, showed the higher residual voltage than that of the RMO. The β-type MnO_2 (Sample no. 4) showed the low output voltage and response, and the negative value of the residual voltage due to the crystalline structure, and the higher electron conductivity compared to other types of MnO_2. And, the λ-type MnO_2 (Sample no. 5; spinel structure [20]) showed the highest output voltage and a good response, but the residual voltage was much higher than that of the RMO. This means that the λ-type MnO_2 is not a good material for the electrolyte in this sensor for the sequential measurements of H_2 concentrations. As a result, the RMO showed the best properties for an H_2 sensor compared to the other crystal types of MnO_2. In addition, the powders of titanium oxide (TiO_2) and aluminium oxide (Al_2O_3) were examined for use as the electrolyte, but the TiO_2 showed no response to the supplied H_2, and the Al_2O_3 showed the unstable output voltages and the responses that depended on the memory effects with previous supply of H_2 in the sequential measurements.

Fig. 2c shows the variation in the impedance of the RMO electrolyte under different conditions. The impedance of the electrolyte in the dry condition showed only the resistance of 1.2 kΩ. This indicates

that the electrolyte made of RMO pellet under dry condition does not work as the H_2 sensor. However, the impedance of the electrolyte in the wet condition showed a large arc in the region from 0.01-100 kHz. In addition, a decrease in the impedance was clearly observed as smaller arcs with increase of the H_2 concentration at the cathode surface. In a past study of electrolytes made of other proton-conductive ceramics operated at 200-900˚C, it was reported that the decrease in the impedance in the low frequency region was due to an increase in the proton conduction in the ceramics used [1]. Thus, the variation in the impedance indicated a change of proton conduction in the wet RMO at room temperature. The previous study [12] reported that the surface of RMO particles produces protonic condition in water. Therefore, the appearance of the proton conductivity in this study is probably due to the homogeneous protonation of the surface of wet RMO particles.

Moreover, a weight decrease of the housing unit in sub-milligram level per hour has been observed after sequential sensor operation (about 6 hours), which was higher when we supplied to the anode nitrogen (100 mL/min) instead of dry air (100 mL/min). This difference can be explained by generation of water on the anode surface as in a typical SOFC reaction (*i.e.* $1/2O_2 + 2H^+ + 2e^- \rightarrow H_2O$), when we supplied dry air (*i.e.* O_2). However, the sensor does not have an external circuit connecting the cathode and the anode for the conduction of electrons (see Fig. 1a). Therefore, the effective double conduction of protons and electrons is expected in the wet RMO electrolyte during the measurement of H_2 concentrations.

4. Conclusions

This study revealed that the high-purity, ramsdellite-crystal type MnO_2 under wet condition showed unique proton conductivity at room temperature, and the hydrogen gas sensor using the electrolyte made of the high-purity, ramsdellite-crystal type MnO_2, enabled the easy in-situ measurements of H_2 concentrations within the wide dynamic range of 0.1-99.9 % at room temperature.

Acknowledgements We thank K. Takeuchi, M. Tsujimoto, Y. Tokuda, and N. Koura for helpful discussions. This work was partly supported by the WPI program from the Ministry of Education, Culture, Sports, Science & Technology of Japan, by the Kurita Water and Environment Foundation, by Kinki Regional Invention Center Foundation and by the Murata Science Foundation. Work at ORNL was supported by the DOE-BES and was managed by UT-Battelle, LLC, for DOE under Contract DE-AC05-00OR22725.

Supporting Online Material Available. This material is available free of charge via the Internet at---.

References

[1] H. Iwahara, H. Uchida, K. Ogaki, H. Nagato, Nernstian Hydrogen Sensor Using $BaCeO_3$ Based, Proton-Conducting Ceramics Operative at 200˚C-900˚C. *Journal of The Electrochemical Society* 138, (1991) 295-299.

[2] G. Lu, N. Miura, N. Yamazoe, High-temperature hydrogen sensor based on stabilized zirconia and a metal oxide electrode. *Sensors and Actuators B: Chemical* 35, (1996) 130-135.

[3] N. Miura, Y. Yan, G. Lu, N. Yamazoe, Sensing characteristics and mechanisms of hydrogen sulfide sensor using stabilized zirconia and oxide sensing electrode. *Sensors and Actuators B: Chemical* 34, (1996) 367-372.

[4] N. Hara, D. D. Macdonald, Development of Dissolved Hydrogen Sensors Based on Yttria-Stabilized Zirconia Solid Electrolyte with Noble Metal Electrodes. *Journal of The Electrochemical Society* 144, (1997) 4152-4157.

[5] K. Katahira, H. Matsumoto, H. Iwahara, K. Koide, T. Iwamoto, A solid electrolyte hydrogen sensor with an electrochemically-supplied hydrogen standard. *Sensors and Actuators B: Chemical* 73, (2001) 130-134.

[6] Y.-C. Liu, B.-J. Hwang, I.-J. Tzeng, Improvements in sensitivity and in anti-aging of Pt/C/Nafion® gases sensors modified by chromium. *Journal of Electroanalytical Chemistry* 533, (2002) 85-90.

[7] M. Matsumiya, F. Qiu, W. Shin, N. Izu, N. Murayama, S. Kanzaki, Thin-film Li-doped NiO for thermoelectric hydrogen gas sensor. *Thin Solid Films* 419, (2002) 213-217.

[8] G. Velayutham, C. Ramesh, N. Murugesan, V. Manivannan, K. S. Dhathathreyan , G. Periaswami, Nafion based amperometric hydrogen sensor. *Ionics* 10, (2004) 63-67.

[9] L. P. Martin, R. S. Glass, Hydrogen Sensor Based on YSZ Electrolyte and Tin-Doped Indium Oxide Electrode. *Journal of The Electrochemical Society* 152, (2005) 43-47.

[10] A. Tomita, Y. Namekata, M. Nagao, T. Hibino, Room-Temperature Hydrogen Sensors Based on an In^{3+}-Doped P_2O_7 Proton Conductor. *Journal of The Electrochemical Society* 154, (2007) 172-176.

[11] N. Miura, H. Kato, N. Yamazoe, T. Seiyama, A Proton Conductor Gas Sensor Operative at Ordinary Temperature. *DENKI KAGAKU*, 50, 10, (1982) 858-859.

[12] H. Koyanaka, K. Takeuchi, C.-K. Loong, Gold recovery from parts-per-trillion level aqueous solutions by a nanostructured manganese oxide-based adsorbent. *Separation and Purification Technology* 43, (2005) 9-15.

[13] S. Iikubo, H. Koyanaka, S. Shamoto, K. Takeuchi, S. Kohara, K. Kodama, C-K. Loong, Local crystal structure of nano-manganese-oxide gold adsorbent. *J. Physics and Chemistry of Solids* 71, (2010) 1603-1608 .

[14] H. Koyanaka, O. Matsubaya, Y. Koyanaka, N. Hatta, Quantitative correlation between Li absorption and H content in Manganese Oxide Spinel λ-MnO_2. *J. Electroanalytical Chemistry*, 559, Nov. (2003) 77-81.

[15] S. Nagakura, Ed., Iwanami Rikagaku Jiten(3rd edition). *Iwanami, Tokyo*, (1974).

[16] C. Fong, B. J. Kennedy, M. M. Elcombe, A powder neutron diffraction study of lambda and gamma manganese dioxide and of $LiMn_2O_4$. *Zeitschrift Fuer Kristallographie* 209, (1994) 941-945.

[17] A. A. Bolzan, C. Fong, B. J. Kennedy, C. J. Howard, Powder neutron diffraction study of pyrolusite, beta-MnO_2. *Aus. J. Chemistry* 46, (1993) 939-944.

[18] L. D. Konddrasev, A. I. Zaslavskii, Stucture of a modification of manganese dioxide. *Izvestiya Akademii Nauk SSSR, Seriya Fizicheskaya*15, (1951) 179-186.

[19] Y. Chabre, J. Pannetier, Structural and electrochemical properties of the proton /gamma-MnO_2. *Prog. Solid St. Chem.* 23, (1995) 1-130.

[20] J. C. Hunter, Preparation of a new crystal form of manganese dioxide: lambda-MnO_2. *J. Solid State Chem.* 39, (1981) 142-147.

Keywords. Hydrogen gas sensor, Hydrogen fuel meter, Manganese dioxide, Double conduction of proton and electron.

Table and Figure captions

Table 1 Comparison of the H_2 sensing properties for various electrolytes made of MnO_2 with different crystal structures. H_2 (99.9%) was supplied at a flow rate of 100 mL/min into the cathode. Dry air was supplied at a flow rate of 100mL/min into the anode. The output voltage was defined as the average voltage generated while supplying H_2 into the cathode for 1 minute. The response was defined as the average of the maximum values of dV/dt. The resistance of each pellet of MnO_2 was measured under dry condition. Residual voltages were measured after purging H_2 from the cathode with N_2 (99.9%) supplied for 1 minute.

Figure 1 Sensor unit and material (**a).** Schematic of the hydrogen gas (H_2) sensor unit. The H_2 was supplied to the upper surface (cathode) of the wet RMO pellet, while dry air was supplied to the

opposite surface (anode) in a housing unit made of polypropylene. The output voltage between the Pt electrodes (100 mesh size, 2 cm diameter) was measured for various H_2 concentrations from 0.1-99.9 % balanced with argon gas (Ar). The internal resistance of the voltage meter was 10 MΩ. The H_2 and dry air flow rates were maintained at 20 mL/min, respectively. (**b).** TEM image of the RMO particles for preparation of the electrolyte.

Figure 2 Properties of the H_2 sensor (**a).** Quick response of the sensor to H_2 supplied to the system, using an H_2 flow rate of 20 mL/min. (**b).** Dependence of the output voltage and the linearity of the response dV/dt on the H_2 concentration for an H_2 flow rate of 20 mL/min. **(c).** Nyquist plots of variation in the H_2 concentration. Distilled water (0.4 mL) was added to the surface of the RMO pellet to provide the wet conditions. The AC frequency was tested from 0.01 Hz to 100 kHz for AC impedance measurements after supplying dry air and H_2 to the cathode (100 mL/min). An applied voltage of 100 mV was used for each measurement.

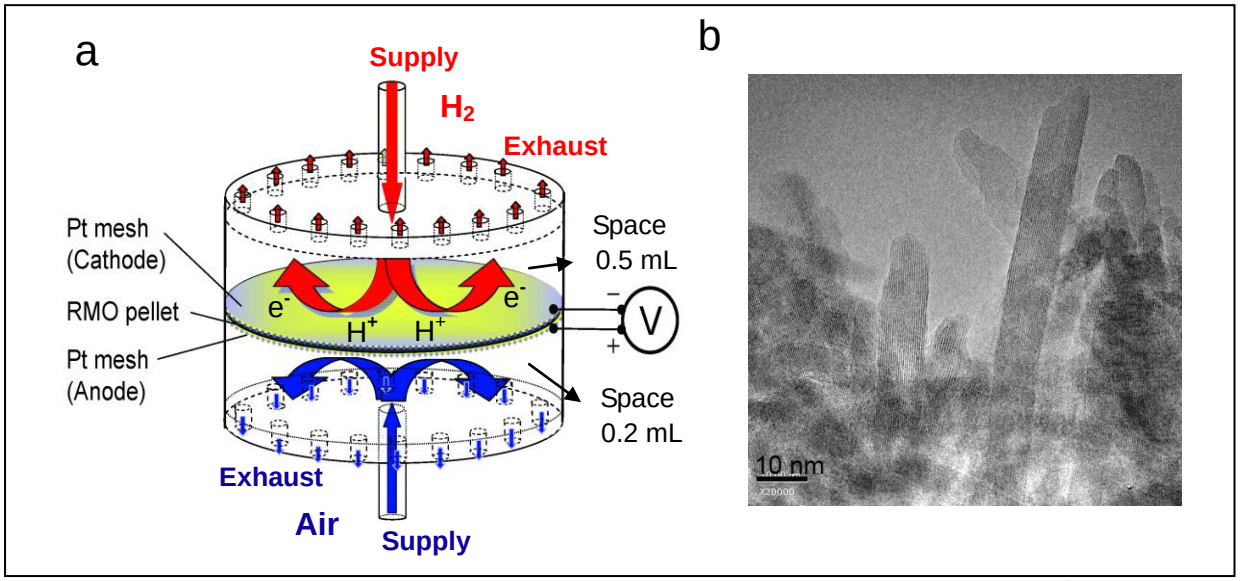

Figure 1

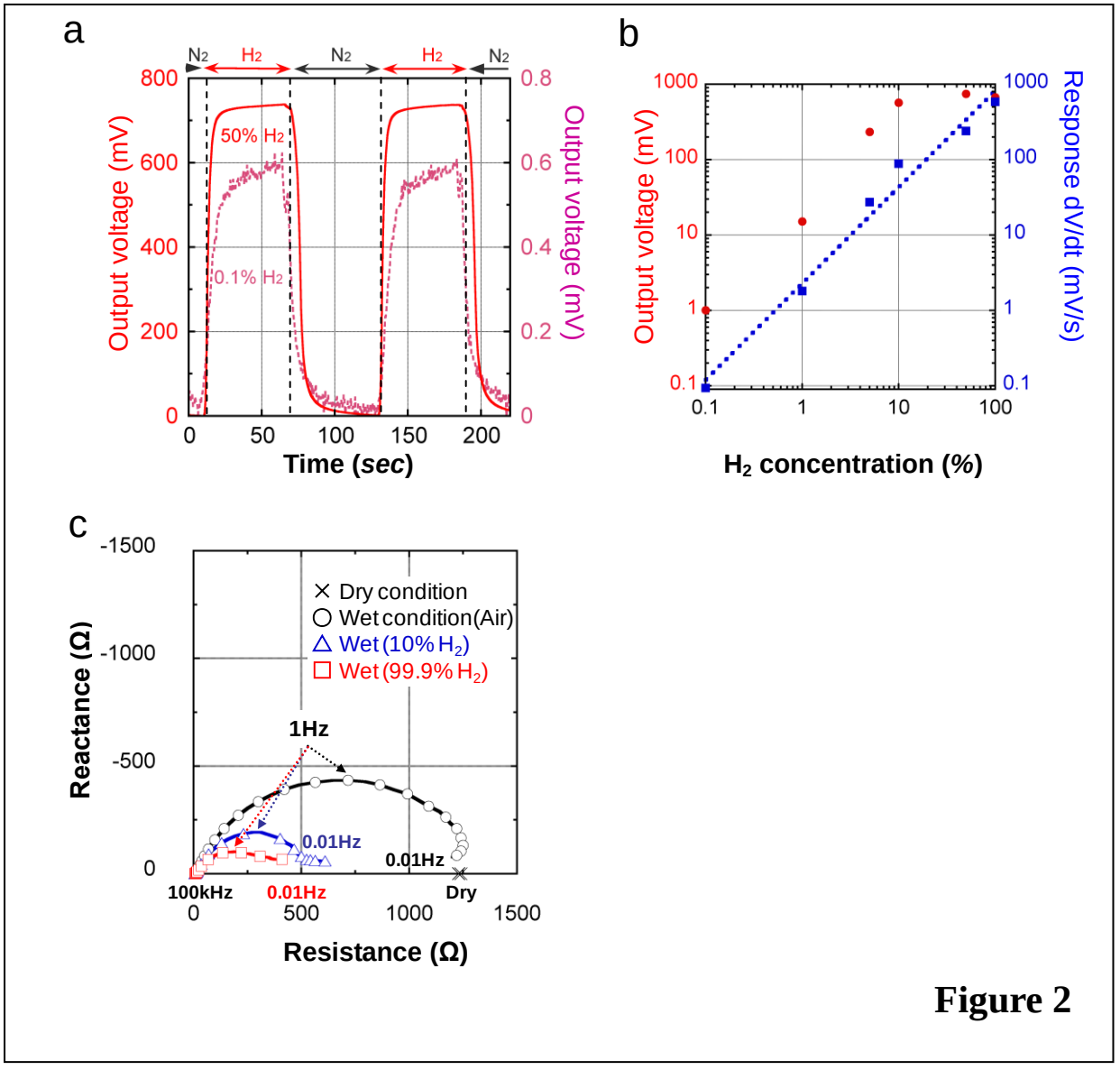

Figure 2

Table 1

	Sample	Output voltage (mV)	Response dV/dt (mV/s)	Residual voltage (mV)
1.	**R-MnO_2**	673.93	536.63	1.99
2.	**β-MnO_2**	94.13	55.07	-4.84
3.	**γ-MnO_2**	375.77	226.09	28.28
4.	**λ-MnO_2**	980.22	479.32	498.08
5.	**CM-MnO_2**	632.43	325.29	128.22

Figure and Table Captions

Figure 1 Sensor unit and material. a Schematic illustration of H_2 gas sensor unit. The RMO powder (0.6g) was processed to a pellet (diameter: 2 cm, thickness: 0.6 mm) of electrolyte in a hydrogen gas (H_2) sensor. The H_2 was supplied to the upper surface (cathode) of RMO pellet, while dry air was supplied to the opposite surface (anode) in a housing unit made of polypropylene. The output voltage between Pt electrodes was measured for various H_2 concentrations of 0.1-99.9 % balanced with argon gas (Ar). The internal resistance of voltage-meter was 10MΩ. Pt meshes (100 mesh size, 2 cm of diameter) were used. Flow amounts of H_2 and dry air were maintained at 20 and 100mL/min, respectively. 0.4 mL of distilled water added onto the surface of RMO pellet before supplying H_2. **b** TEM image of the nanometer scale of ramsdellite-crystal structure of MnO_2 (RMO) particles for preparation of electrolyte. Meso-space between the aggregated nano-particles was estimated at about 20 nm, which is large enough for the infiltration of air and water molecules. The surface area was found to be 71.2 m^2/g.

Figure 2 Properties of H_2 sensor. a Quick response with H2 supply to the sensor system, flow amount of H_2 was 20 mL/min. **b** Dependence of output voltage mV and linearity of response dV/dt mV/sec on H_2 concentration. Flow amount of H_2 was 20 mL/min. **c** Nyquist plots on variation of H_2 concentration. 0.4 mL of distilled water

added onto the surface of RMO pellet to prepare the wet condition. The AC frequency was tested from 0.01 Hz to 100 kHz for AC impedance measurements after supplying dry air and H_2 to the cathode (100 mL/min). Applied voltage of 100 mV was loaded for each measurement.

Table 1 Comparison of sensoring properties of H_2 in various electrolytes which made of different crystal structures of MnO_2. 99.9% of H_2 was supplied with flow amount of 100mL /min into the cathode. Residual voltages were measured after purging H_2 from cathode by supplying N_2 gas. Output voltage was defined as the average voltage generated while supplying H2 into cathode for 1 minute. Response was defined as average of the maximum value of dV/dt.

SUPPLEMENTARY INFORMATION

Hydrogen gas sensor using nano-scale manganese dioxide

Yoshikatsu Ueda[1], Alexander I. Kolesnikov[2], and Hideki Koyanaka[3*]

[1]*Research Institute for Sustainable Humanosphere, Kyoto university, Kyoto, 611-0011, Japan*

[2]*Neutron Scattering Sciences Division, Oak Ridge National Laboratory, Oak Ridge, TN 37831-6473, USA*

[3]*Institute for Integrated Cell-Material Sciences, Kyoto University, Kyoto, 606-8501, Japan*

Index

ADDITIONAL REFERENCES

1. System of H_2 gas sensor in this study

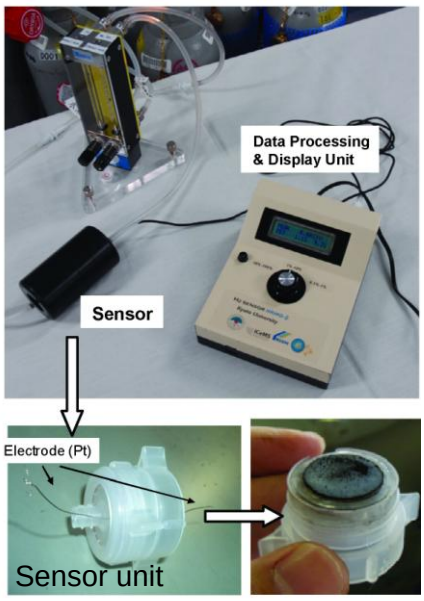

Figure 3. Photographs of the H_2 gas sensor system.

The experimental setup was showed in **Fig. 3**, where the couple of Pt meshwork attached onto the wide pellet surfaces worked as electrodes and also as a catalyst for the H_2 ---> $2H^+ + 2e^-$ dissociation. This system is conceptually similar to SOFC[15]. The H_2 gas was supplied to the upper surface, while air was introduced onto the other side. We measured the voltage generated between the Pt electrodes as a function of the H_2 concentration used. The flow rate of dry air was fixed at 100 ml/min, and that of H_2 was controlled as 10, 20, 50, and 100 ml/min. The voltage between the Pt electrodes was measure for various H_2 concentrations of 0.1-99.9 % prepared with Ar balance. The temperature of the pellet was maintained at room temperature. In addition, a titanium oxide TiO_2 (Wako 325-38392) and an activated Al_2O_3 (Wako 010-01525) were tested for pellets of the reference compared to MnO_2 pellets.

2. X-ray diffraction analysis of manganese dioxides tested.

We determined crystal structures of MnO_2 by X-ray diffraction (XRD) patterns. The XRD pattern of the RMO corresponding to the TEM image in Fig. 1b was displayed at the top of **Fig. 4a**. The XRD peak positions almost coincided with the positions of the crystalline ramsdellite[16] (shown as ticks at the bottom of Fig. 4a). The Jahn-Teller distortion factor[16] (JTDF) for the sample was 0.957, which was calculated using d-values $d_{(210)}$=2.424 Å, $d_{(211)}$=2.127 Å and $d_{(610)}$=1.359 Å. This result indicated a high purity of the crystal structure as ramsdellite. **Figs. 4b-e** showed X-ray diffraction patterns of other crystal types of MnO_2 tested in this study. The commercial MnO_2 was Wako 134-12301.

a)

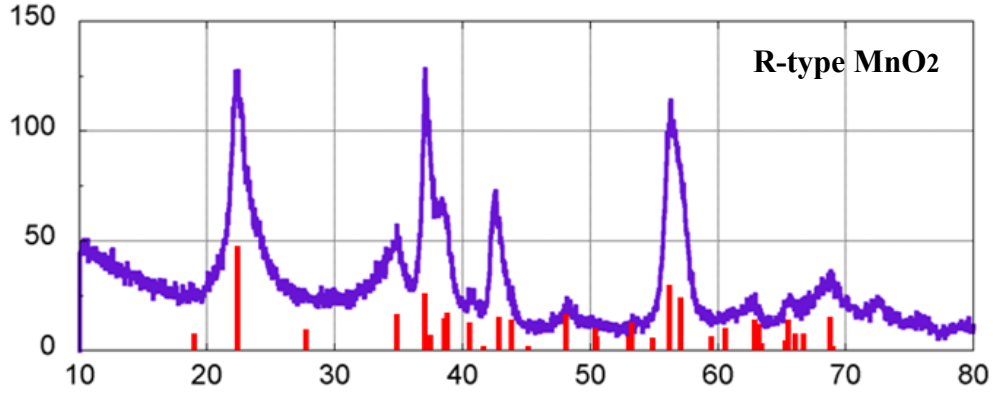
R-type MnO2
150
100
50
0
10
20
30
40
50
60
70
80

b)

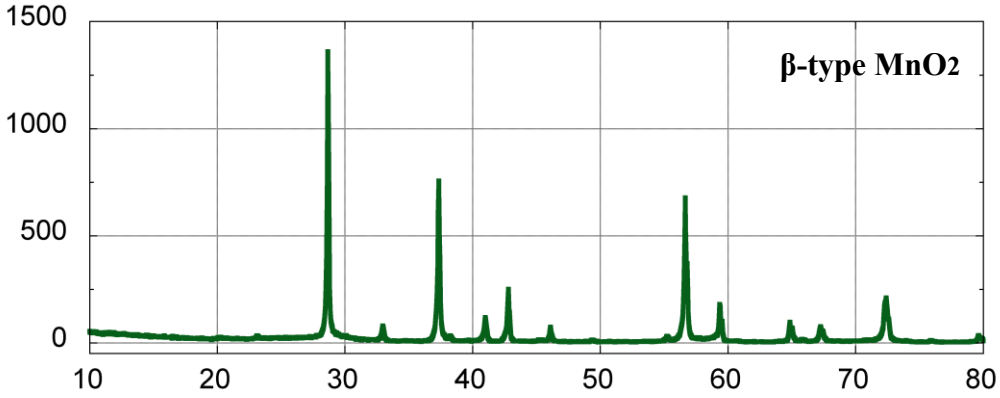
β-type MnO2
1500
1000
500
0
10
20
30
40
50
60
70
80

c)

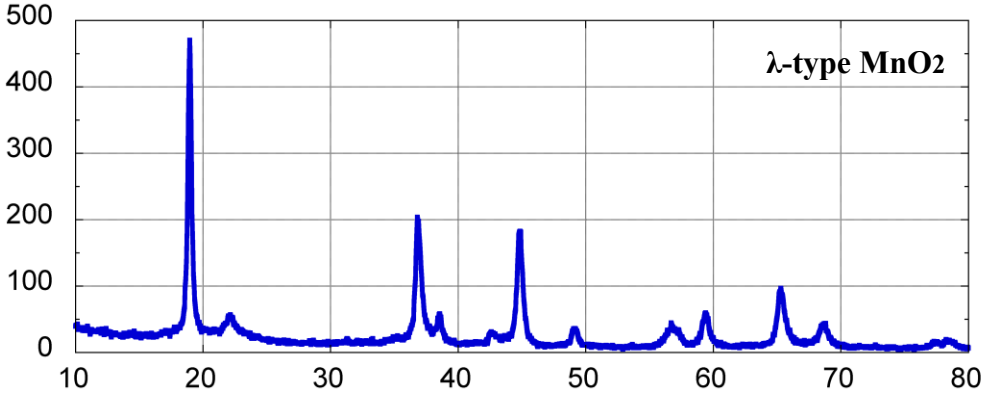
λ-type MnO2
500
400
300
200
100
0
10
20
30
40
50
60
70
80

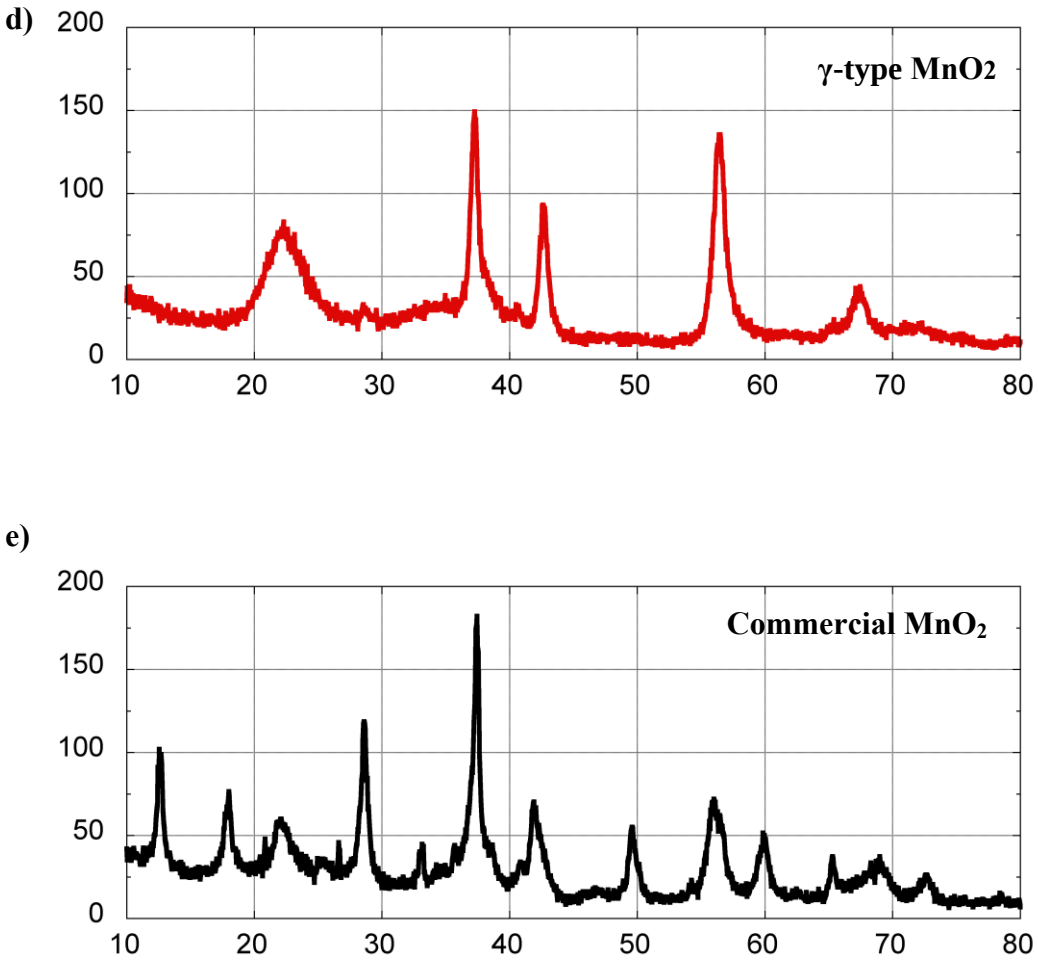

Figure 4 X-ray diffraction patterns of MnO_2 : (a) R-type[17], (b) β-type[18], (c) λ-type [19,20], (d) γ-type[16], and (e) commercial MnO_2 samples used.

ADDITIONAL REFERENCES

15. K. Takeuchi, Y. Ishida , K. Kasuya , R. Tai , H. Koyanaka , K. Ui , and N. Koura, Development of novel anodic catalyst for solid oxide fuel cell operated at intermediate-temperature direct utilizing of dimethylether fuel, *Electrochemistry*, **75**, No. 10, (2007)

16. Chabre, Y. and Pannetier, J. Structural and electrochemical properties of the proton /gamma-MnO_2. *Prog. Solid St. Chem.* **23**, 1-130 (1995).

17. Rossouw, M. H., Liles, D. C., Thackeray, M. M., David, W. I. F., Hull, S. Alpha manganese dioxide for lithium batteries: A structural and electrochemical study. *Materials Research Bulletin* **27**, 221-230 (1992).

18. Bolzan, A. A., Fong, C., Kennedy, B. J., Howard, C. J. Powder neutron diffraction study of pyrolusite, beta-MnO_2. *Aus. J. Chemistry* **46**, 939-944 (1993)

19. Hunter, J. C. Preparation of anew Crystal Form of Manganese Dioxide: lambda-MnO_2. *J. Solid State Chem*. **39**, 142-147 (1981).

20. Koyanaka, H, Matsubaya,O., Koyanaka,Y., and Hatta ,N. Quantitative correlation between Li absorption and H content in Manganese Oxide Spinel λ-MnO_2, *J. Electroanalytical Chemistry,* **559**, Nov p.77-81(2003)